

Concept and computational design for a bioartificial nephron-on-a-chip

E. WEINBERG^{1,2}, M. KAAZEMPUR-MOFRAD³, J. BORENSTEIN²

¹ Department of Mechanical Engineering, Massachusetts Institute of Technology, Cambridge, Massachusetts

² Draper Laboratory, Cambridge, Massachusetts - USA

³ Department of Bioengineering, University of California Berkeley, Berkeley, California - USA

ABSTRACT: A MEMS-based, (Micro Electro Mechanical System) bioartificial device is proposed for replicating the function of a single nephron. Consistent with the anatomy and physiology of humans, our device has 3 distinct sections, replicating the function of the glomerulus, the proximal tubule, and the loop of Henle. Construction of a bioartificial loop of Henle in particular requires control of diffusion-scale features. The proposed device can be built using existing microfabrication technologies and populated with various renal cell types. A computational model is also developed to analyze the coupled, multi-phase mass transport in this system. Using the model, a design is generated with flow and solute transport properties matching those of the human nephron (Int J Artif Organs 2008; 31: 508-14)

KEY WORDS: Bioartificial MEMS-based device, Computational modeling, Nephron, Renal replacement

INTRODUCTION

The human kidney is composed of approximately 1.2 million individual nephrons working in parallel. Each nephron is intricate in geometry and function. Here we describe the most basic elements. The nephron can be most simply divided into 3 main components. Blood flowing into the nephron first enters the glomerulus, where the blood is filtered by passive mechanical filtration, retaining cells and large proteins. From there, blood and filtrate flow to the proximal tubule. In the proximal tubule, large amounts of solute and fluid are actively reabsorbed. Finally, the blood and filtrate flow to the loop of Henle and associated collecting ducts. In this part of the nephron, active pumping, osmosis, and diffusion combine to reabsorb almost all of the remaining filtrate fluid and output highly concentrated waste urine. The system is very efficient in its ability to remove large amounts of urea from the blood without removing large amounts of fluid (1). Existing approaches to the engineering of kidney devices have replicated parts of the nephron function but not all, and thus have not been able to match the efficiency of the functional nephron.

Several remarkable efforts have been made to artificially replicate kidney function (2). In dialysis, either hemodialysis or hemofiltration, blood is pumped past a porous membrane. Waste clearance occurs mainly by diffusion in hemodialysis and by convection in hemofiltration or hemodiafiltration. Dialysis has had an enormous clinical impact over the past 3 decades (3), as well as steadily improving patient outcomes. More recently, Humes et al have developed bioartificial kidney devices which have entered human trials (4, 5). These devices add proximal tubule cells to a dialysis filter to achieve reabsorption and add metabolic activity to the device (6). Dialysis essentially replicates the function of the glomerulus, and the bioartificial kidney devices replicate the function of the glomerulus and proximal tubule. Other technologies are in earlier stages of development. Gura's group has made progress in miniaturizing and optimizing the dialysis equipment, possibly reducing the overall package to a wearable size (7). Leonard et al have made progress in membraneless transport that may lead to improved dialysis systems (8). Nissenson et al have proposed a device that, using artificial transport channels, replicates renal glomerulus and tubule function (9).

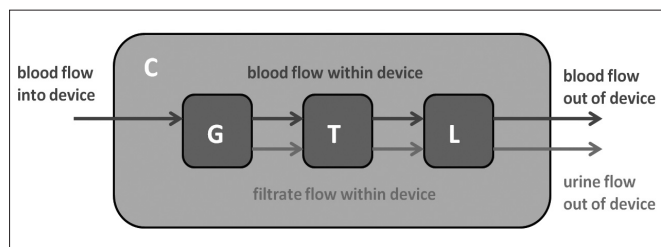


Fig. 1 - Schematic overview of nephron device.

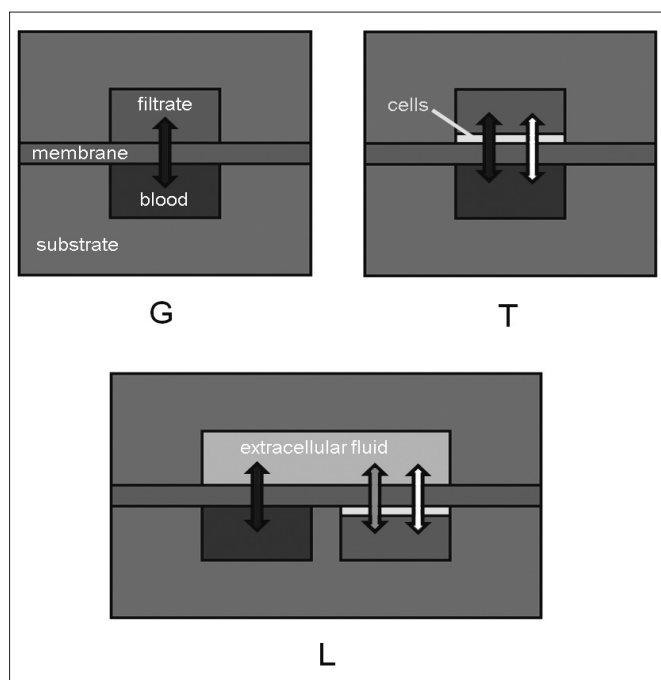


Fig. 2 - Schematic cross-sections of the 3 functional units. Black arrows denote passive transport; white arrows denote cell-mediated active transport.

Unlike renal replacement technologies in existence or under development, the nephron is able to filter blood with exceptional efficiency: less than 1% of the blood entering the nephron is lost as waste, and no dialysate fluid or external pumping system is necessary. The nephron achieves this performance using the 3-step system of the glomerulus, tubule, and loop of Henle in series. An artificial device that replicates this 3-step system can potentially match the efficiency of the nephron, and thus lead to compact and wearable devices that other technologies cannot.

The loop of Henle and collecting duct produce concen-

trated urine by using a countercurrent exchange mechanism. This mechanism requires looping geometries with features on the diffusion scale. These features, along with porous regions to allow communication between compartments, can be readily produced using microfabrication. Many groups have demonstrated various methods for creating microfabricated devices and incorporating biological elements. Borenstein et al have demonstrated the ability to fabricate multilayer devices from various polymers, incorporating porous membranes between layers (10, 11). In this paper, we design a nephron device that can be built using 2 microfabricated layers connected by a porous membrane.

A number of cell types exhibiting a wide range of functions are found in the nephron. To replicate the nephron in silico, functional cells will have to be located and oriented correctly in the device. A great deal of study and success has been reported controlling proximal tubule cells in relation to the existing bioartificial kidney devices (12, 13). Progress is being made in investigating and controlling the differentiation and function of cell types found in the loop of Henle and collecting ducts (14-19). Additional aspects, such as the role of circulating hormones, such as antidiuretic hormone (ADH) released by the pituitary gland in modulating tubule permeability to water, will ultimately be important for the design and function of the bioartificial nephron-on-a-chip, but are beyond the scope of this initial proof-of-concept.

In this paper, we design and perform computational analysis of a nephron device that can be fabricated on a single multilayered polymer construct. This device replicates the 3-step system of filtration found in the functioning nephron. We introduce a numerical scheme to simulate the complex flow behavior of the nephron, and use this scheme to design the full device. This design is intended to be a starting point for efforts to tissue engineer first individual elements of this device and then create a functional bioartificial nephron.

METHODS

Design concept

Our research group has experience building microfabricated devices with multiple layers separated by membranes (10, 11, 20). The goal of the present work is to produce a design for a nephron device that mostly can

be built simply using existing methods. The complete device has 4 components: the glomerulus (G), the tubule (T), the loop of Henle (L), and the connector (C). G, T, and L replicate the functions of the nephron and C interfaces those with each other and with the blood and waste streams. A schematic of the device is shown in Figure 1.

In our simplest conception, the nephron device is fabricated from 2 microfabricated layers separated by a membrane. Cross-sectional schematics of each of the 3 functional components are shown in Figure 2. The G and T units can be composed of straight channels, while the L unit requires countercurrent loops (see Fig. 3). Schematics of the design for each component are shown in Figure 3. The looping geometry of L allows countercurrent transport. The design length L for each component is illustrated in Figure 3.

T requires renal proximal tubule cells, and L requires a number of different cell types: namely, cells of the descending thin limb, ascending thin limb, thick ascending limb, cortical collecting duct, and medullary collecting duct. Each cell type has distinct transport properties and characteristics (see Tab. I).

Numerical model

To design this device, we developed a numerical model at Matlab (The Mathworks, Natick, MA, USA) that is suited to simulating the multiphase fluid and particle transport. A simple rectilinear mesh is created to represent the basic geometries for the G, T, and L units (see Fig. 4). Our model calculates the fluid and solute motion on those meshes in 2 separate steps.

The first solution step calculates fluid motion using a network solution. In this solution, pressures and flows are calculated in a manner analogous to that commonly used to find voltages and currents in an electrical network (22).

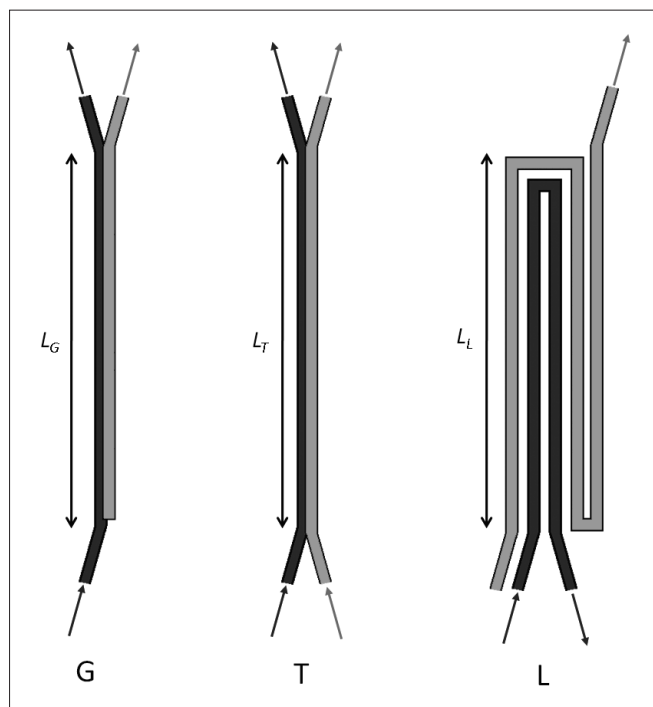


Fig. 3 - Schematics of overhead view of wafer for each component. Arrows represent flow directions for blood (black arrows) and filtrate (grey arrows) at component inlets and outlets.

The volumetric flux from mesh point 1 to mesh point 2 is given by the equation:

$$\phi_v = L_v(P_1 - P_2) - L_v \sum_i \sigma_i (\pi_{1i} - \pi_{2i})$$

where L_v is the hydraulic conductivity between the 2 points, P_1 and P_2 are the hydrostatic pressures at points 1 and 2, σ_i is the reflection coefficient of solute i , π_{1i} and π_{2i} are the osmotic pressures at points 1 and 2 due to a concentration gradient in solute i (23). If the 2 mesh points are in the same fluid vessel, L_v is simply deter-

TABLE I - TRANSPORT PROPERTIES OF CELLS REQUIRED IN NEPHRON DEVICE

Location	Active NaCl transport	Passive permeabilities		
		NaCl	Urea	H ₂ O
Proximal tubule (T)	+++	+		+++
Descending thin limb (DTL)		+	+	+++
Ascending thin limb (ATL)		+++		
Thick ascending limb (TAL)	+++	+		
Cortical collecting duct (CCD)	+	+		
Medullary collecting duct (MCD)	+	+	++	+

More + marks signifies higher permeability; no + marks signifies impermeability.

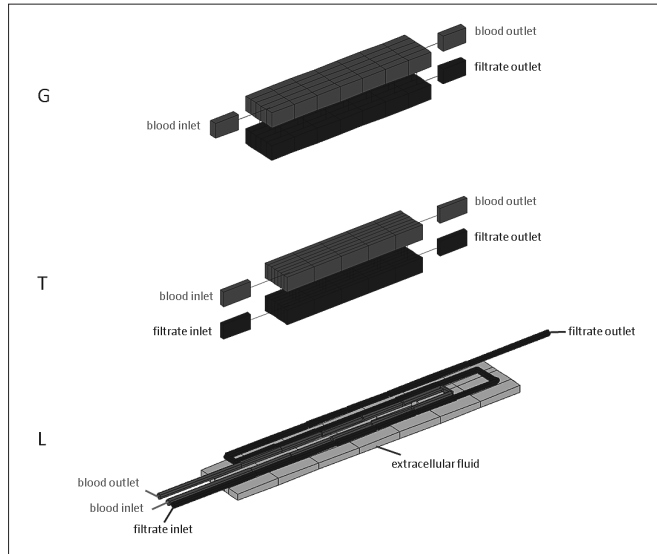


Fig. 4 - Meshes generated for each device component (not to scale).

TABLE II - SOLUTE CONCENTRATIONS AT DEVICE INLET

Solute	Concentration (mmol/L)
Albumin	0.6
Urea	2.0
Na+	140
Cl-	100

TABLE III - DESIGN REQUIREMENTS FOR GLOMERULUS (G), TUBULE (T), AND LOOP OF HENLE (L) DEVICE COMPONENTS

Device component	Design requirement
G	15%-20% filtration fraction
T	65%-70% of filtrate reabsorbed
L	200-400 mM urea concentration in urine

mined from the pressure-flow relation for a rectangular vessel (24). If there is a membrane between the 2 points, L_v is determined from the Darcy permeability of the membrane. L_v of a membrane may be modified by a polarization layer that develops when there is a high fluid flux through the membrane. Moussy gives a method for calculating this effect (21, 25). The hydrostatic pressures are calculated using nonlinear fits to experimental data (21, 25). A matrix solution of Equation 1 gives the pressures and flows throughout the system.

Once the flow behavior is known, the solute motion can be calculated. Flux of solute j from point 1 to point 2 is given by

$$\phi_j = \bar{c}_j(1 - \sigma_i)\phi_v + \frac{D_j}{\Delta x}(C_{1j} - C_{2j}) + \phi_{Aj}$$

where \bar{c}_j is a representative concentration, D_j is the diffusivity, Δx is the distance between point 1 and 2, C_{1j} and C_{2j} are the concentrations of the solute at points 1 and 2, and ϕ_{Aj} is the flux due to active transport (23). Diffusivity in the blood is calculated including the effect of mixing by the red blood cells (25). Concentration at a point P is updated by

$$C_P^{t+\Delta t} = C_P^t + \left(\frac{A\phi_j}{V}\right)\Delta t$$

where Δt is the time step, V is the volume of the region surrounding point P , and A is the area of the interface between adjacent volumes. Concentrations at all points in the mesh are updated by applying Equation 3 along all connections in the mesh. This method for updating concentrations is first-order and introduces significant numerical smearing of transient behavior (26). We use this method only to analyze steady-state conditions.

G, T, and L are modeled separately. Four solutes were considered throughout: albumin, urea, and Na^+ , and Cl^- . The concentration inlet conditions are applied at the inlet to G, where all solutes are assumed to have concentrations typical of normal blood (see Tab. II). The outlet concentrations of G are then applied as inlet conditions to T and outlet conditions of T applied as inlet conditions to L. Flow rate boundary conditions are applied in each case. Inlet blood flow rate to G is set at 0.025 ml/hour, the flow rate to a single nephron based on a kidney comprising 1.2 million nephrons receiving a total flow rate of 0.5 l/min (1). To allow this flow to be driven by physiological blood pressure, we would like the total pressure drop across the device to be approximately 120 mm Hg. Simple design specifications were defined for each section of the device to replicate the behavior of the physiological nephron. These design specifications are listed in Table III. For each device component, the simulation was run to steady-state, then the geometry was modified and simulation run to steady-state again, iteratively until the design requirements were met.

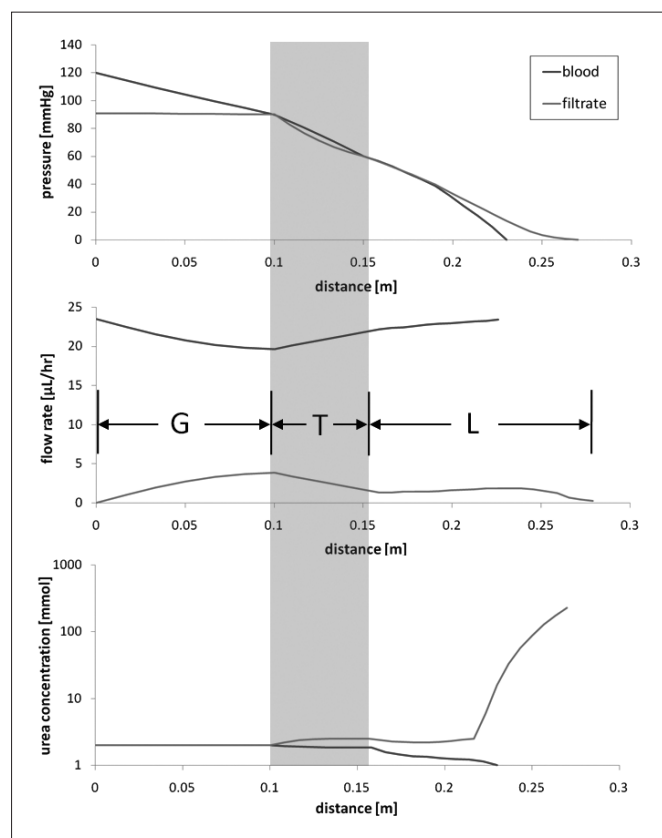


Fig. 5 - Transport behavior for complete device. Distance refers to position along flow path. Gray region denotes tubule (T) component of device. Note that urea concentration is plotted on a logarithmic scale.

RESULTS

Rectilinear meshes were generated for each case and are illustrated in Figure 4. All simulations ran to steady-state convergence. Geometries were iteratively adjusted for each component until the design requirements listed in Table III were met. Results of the individual simulations were then combined to give the transport behavior for the whole device, shown in Figure 5. The simulations display the basic behavior of each component: filtration of the glomerular unit, reabsorption in the tubule, and the large increase in urea concentration in the loop of Henle (see Fig. 5). The large jump in the urea concentration occurs as the filtrate flows in the collecting duct, reabsorbing fluid and exchanging NaCl for urea. The inner medullary collecting duct has as 1 of its principal functions the addition of urea to papillary interstitial spaces; the other is the

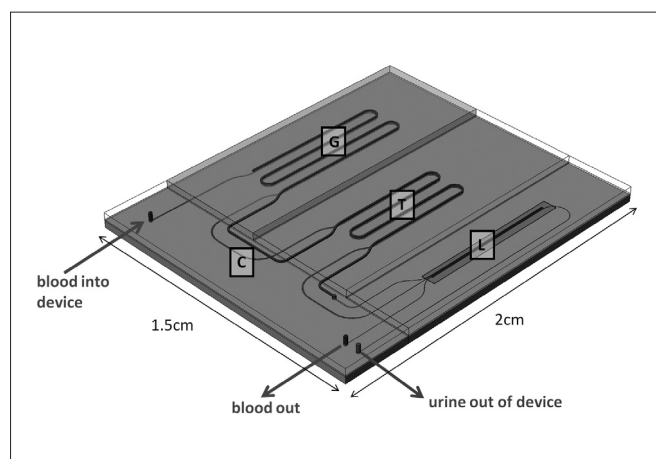


Fig. 6 - Overall view of complete device design.

TABLE IV - DESIGN DIMENSIONS

	Component		
	G	T	L
L, cm	10.00	5.30	4.00
W, μm	70.00	35.00	25.00
D_B , μm	40.00	40.00	25.00
D_F , μm	50.00	15.00	25.00

L is the dimension in Figure 3, W is the width of the flow channels, and D_B and D_F are the depths of the blood and filtrate side, respectively. G: glomerulus; L: loop of Henle; T: tubule.

formation of urine that is concentrated as much as possible (27). The role performed by the collecting duct in urea transport and urine concentration is clearly essential and must ultimately be incorporated into the bioartificial nephron on a chip device. The current design has the desired total flow rate and end-to-end pressure drop. Final geometry values are listed in Table IV. For each component, L is the dimension shown in Figure 3, D_B is the depth of the blood channel, D_F is the depth of the filtrate channel, and W is the width of both the blood and filtrate channels. Using the device dimensions for the components, we created a complete design of the nephron device. This design includes components C, G, T, and L. It is composed of 2 microfabricated layers “sandwiched” around a dialysis membrane. Component C includes interfaces for external tubing. An overall view of this design is shown in Figure 6.

CONCLUSIONS

In this paper, we have created an initial design for a MEMS-based bioartificial nephron. The mechanical structure of this device can be readily constructed using existing microfabrication technologies that allow for diffusion-scale structures, enabling the creation of a loop of Henle in this device. With the loop of Henle, in combination with components to replicate glomerulus and proximal tubule, this device promises to replicate the full filtration and reabsorption behavior of a physiological nephron. This design represents a significant step over current artificial and bioartificial technologies that can replicate glomerular and proximal tubule function, but not filter waste with nearly the efficiency of the nephron. While significant

challenges await in the areas of culture and control of the various cell types needed for this device, the design presented here can potentially enable a large improvement in bioartificial kidney technology.

Conflict of interest statement

The authors have no conflict to report.

Address for correspondence:

Jeffrey T. Borenstein, PhD
Distinguished Member of Technical Staff
Director, Biomedical Engineering Center
Draper Laboratory
Mail Stop 32
555 Technology Square
Cambridge, MA 02139, USA
e-mail: jborenstein@draper.com

REFERENCES

1. Koeppen B, Stanton B. Renal physiology; 3rd ed. St Louis, MO: Mosby, 2001.
2. Reyez-Ortiz V, Mofrad M, Weinberg E, Borenstein J. Renal replacement technologies. In: Khademhosseini A, Toner M, Borenstein J, eds. Micro- and nanoengineering of the cell microenvironment: technologies and applications. Norwood, MA: Artech House Publishing, 2007.
3. Galletti P, Colton C, Lysaght M. Artificial kidney. In: Bronzino J, ed. The biomedical engineering handbook. Boca Raton, FL: CRC Press, 1995.
4. Humes HD, Paganini EP, Weitzel WF, Swaniker FC, Bartlett RH. Clinical results of a phase I/II trial of the bioartificial kidney (BAK) in intensive care unit (ICU) patients with acute renal failure (ARF). *J Am Soc Nephrol* 2003; 14: 454-61.
5. Humes HD, Weitzel WF, Bartlett RH, Swaniker FC, Paganini EP, Luderer JR, . Initial clinical results of the bioartificial kidney containing human cells in ICU patients with acute renal failure. *Kidney Int* 2004; 66: 1578-88.
6. Humes HD, MacKay SM, Funke AJ, Buffington DA. Tissue engineering of a bioartificial renal tubule assist device: in vitro transport and metabolic characteristics. *Kidney Int* 1999; 55: 2502-14.
7. Gura V, Beizai M, Ezon C, Polaschegg HD. Continuous renal replacement therapy for end-stage renal disease: the wearable artificial kidney (WAK). *Cardiovascular disorders in hemodialysis. Contrib Nephrol* 2005; 149: 325-33.
8. Leonard EF, Cortell S, Vitale NG. Membraneless dialysis: is it possible? *Cardiovascular disorders in hemodialysis. Contrib Nephrol* 2005; 149: 343-53.
9. Nissenson AR, Ronco C, Pergamit G, Edelstein M, Watts R. The human nephron filter: toward a continuously functioning, implantable artificial nephron system. *Blood Purif* 2005; 23: 269-74.
10. Borenstein JT, Weinberg EJ, Orrick BK, Sundback C, Kaazempur-Mofrad MR, Vacanti JP. Microfabrication of three-dimensional engineered scaffolds. *Tissue Eng* 2007; 13: 1837-44.
11. Borenstein JT, Terai H, King KR, Weinberg EJ, Kaazempur-Mofrad MR, Vacanti JP. Microfabrication technology for vascularized tissue engineering. *Biomed Microdevices* 2002; 4: 167-75.
12. Humes HD, Fissell WH, Weitzel WF. The bioartificial kidney in the treatment of acute renal failure. *Kidney Int* 2002; 61 (Suppl): S121-5.
13. Fissell WH. Developments towards an artificial kidney. *Expert Rev Med Devices* 2006; 3: 155-65.
14. Bourgeois S, Rossignol P, Grelac F, Chalumeau C, Klein C, Laghmani K. Differentiated thick ascending limb (TAL) cultured cells derived from SV40 transgenic mice express functional apical NHE2 isoform: effect of nitric oxide. *Pflugers Arch Eur J Physiol* 2003; 446: 672-83.
15. Grunewald RW, Reisse CH, Muller GA. Characteristics of urea transport of cells derived from rabbit thick ascending limb of Henle's loop. *Kidney Int* 1998; 54: 152-9.
16. Jans F, Vandenabeele F, Helbert M, Lambrichts I, Ameloot M, Steels P. A simple method for obtaining functionally and morphologically intact primary cultures of the medullary thick ascending limb of Henle's loop (MTAL) from rabbit kidneys. *Pflugers Arch Eur J Physiol* 2000; 440: 643-51.

17. Qi W, Johnson DW, Vesey DA, Pollock CA, Chen XM. Isolation, propagation and characterization of primary tubule cell culture from human kidney. *Nephrology* 2007; 12: 155-9.
18. Terryn S, Jouret F, Vandenebeele F, Smolders I, Moreels M, Devuyst O. A primary culture of mouse proximal tubular cells, established on collagen-coated membranes. *Am J Physiol Renal Physiol* 2007; 293: F476-85.
19. Vandewalle A. Immortalized renal proximal and collecting duct cell lines derived from transgenic mice harboring L-type pyruvate kinase promoters as tools for pharmacological and toxicological studies. *Cell Biol Toxicol* 2002; 18: 321-8.
20. Borenstein J, Weinberg E, Vacanti J, Mofrad M. Microfabrication for vascular engineering. In: Khademhosseini A, Toner M, Borenstein J, eds. *Micro- and nanoengineering of the cell microenvironment: technologies and applications*: Norwood, MA: Artech House Publishing, 2007.
21. Moussy Y. Bioartificial kidney: Part II: a convective flow model of a hollow fiber bioartificial renal tubule. *Biotechnol Bioeng* 2000; 68: 153-9.
22. Weinberg E, Mofrad M, Borenstein J. Numerical model of flow in distensible microfluidic network. In: Bathe K, ed. *Computational fluid and solid mechanics*. New York, NY: Elsevier Science, 2003; 1569.
23. Weiss T. *Cellular biophysics*. Cambridge, MA: Bradford Books, 1996.
24. Papanastasiou T, Georgiou G, Alexandrou A. *Viscous fluid flow*. Boca Raton, FL: CRC Press, 2000.
25. Moussy Y. Bioartificial kidney: Part I: theoretical analysis of convective flow in hollow fiber modules: application to a bioartificial hemofilter. *Biotechnol Bioeng* 2000; 68: 142-52.
26. Leveque R. *Finite volume methods for hyperbolic equations*. Cambridge, UK: Cambridge University Press, 2002.
27. Kokko JP. The role of the collecting duct in urinary concentration. *Kidney Int* 1987; 31: 606-10.